J Intell Robot Syst (2016) 84:639–664
DOI 10.1007/s10846-015-0328-6

Rapid Prototyping of a Fixed-Wing VTOL UAV for Design Testing

Yucel Orkut Aktas · Ugur Ozdemir · Yasin Dereli · Ahmed Farabi Tarhan · Aykut Cetin · Aslihan Vuruskan · Burak Yuksek · Hande Cengiz · Serkan Basdemir · Mesut Ucar · Murat Genctav · Adil Yukselen · Ibrahim Ozkol · Metin Orhan Kaya · Gokhan Inalhan

Received: 15 December 2014 / Accepted: 28 December 2015 / Published online: 18 February 2016

Abstract Over the last decade, the share of civilian Unmanned Aerial Vehicles (UAVs) in the general UAV market has steadily increased. These systems are being used more and more for applications ranging from crop monitoring to the tracking air emissions in high-pollution areas. Most civilian applications require UAVs to be low cost, portable, and easily packaged while also having Vertical Take-off and Landing (VTOL) capability. In light of this, the TURAC was designed, a VTOL Tilt Rotor UAV with these capabilities. Mathematical and CFD analyses were performed iteratively in order to optimize the design, but testing in actual conditions were needed. However, as with such an iterative design process, the manufacturing process costs, including different molds for each design, can be exorbitant. In addition, once an imperfection in the design is encountered, making design modifications on the full scale UAV prototype is difficult and expensive. Therefore, a cheap, rapid, and easily reproducible prototyping methodology is essential. In this study, the end result of an iterative design process of TURAC is presented. In addition, a low-cost prototyping methodology is developed and its application is demonstrated in detail. The ground and flight tests are applied on a fully functional prototype and the results are given.

Keywords Low-cost prototyping · VTOL UAV · Flight testing

G. I. is the PI of the associated Research Project.

Y. O. Aktas (✉) · U. Ozdemir · Y. Dereli · A. F. Tarhan · A. Cetin · A. Vuruskan · B. Yuksek · A. Yukselen · I. Ozkol · M. O. Kaya
Istanbul Technical University, 34469, Istanbul, Turkey
e-mail: orktaktas@gmail.com

H. Cengiz · S. Basdemir · M. Ucar · M. Genctav
HAVELSAN A.S., M. Kemal Mah. 2120. Cad. No:39, 06510, Cankaya, Ankara, Turkey

G. Inalhan
Istanbul Technical University, Faculty of Aeronautics and Astronautics, 34469, Istanbul, Turkey
e-mail: inalhan@itu.edu.tr

1 Introduction

Nowadays, civil Unmanned Aerial Vehicles (UAVs) are actively utilized for civilian purposes such as monitoring traffic and wildlife or conducting geological or mining research. UAVs with features such as vertical take-off, landing, and hovering capability, easy portability and the ability to work with different kinds of payloads have become promint. A civilian Tilt Rotor VTOL UAV with these features was designed, called the TURAC [1]. As shown in Fig. 1 during a hover test, the TURAC UAV has one main co-axial rotor in the rear and two tilt rotors in the front. The the TURAC was designed by a research group with

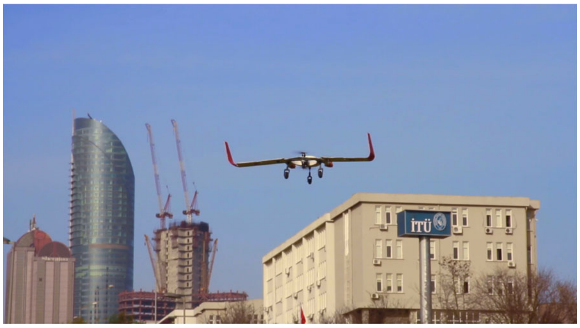

Fig. 1 TURAC VTOL tilt rotor UAV

extensive background in various UAVs such as tilt-rotor VTOL UAVs [1], tailless UAVs [2], tailsitter UAVs [3], and conventional fixed wing and rotary UAVs. We refer the reader to [1] for an extensive treatment of the civilian VTOL mini-UAV market and its needs, the potential advantages of the TURAC, and how the TURAC compares to other similar vehicles.

Most civilian applications require UAVs to be low cost, portable, and easily packaged while also having Vertical Take-off and Landing (VTOL) capability. In light of this, the TURAC was designed, a VTOL Tilt Rotor UAV with these capabilities. We again refer the reader to [1] for an extensive treatment of the TURAC design process. In addition, mathematical and CFD analyses were performed [4] iteratively in order to optimize the TURAC design. Specifically the dynamic modeling and CFD analysis of TURAC, including the important transition flight regime is performed. The TURAC includes different flight phases such as hovering, transition from hovering to cruise and vice versa. Given the inherently unstable flight modes, TURAC UAV relies heavily on autopilot hardware and algorithms [5–7] for flight. We refer the reader to [8] for more detailed information on the avionics and the associated ground station.

Even though the numerical and modeling analysis play a crucial role in conceptual design, actual prototyping and in-flight validation is key to any successful design. However, during an iterative design process, the manufacturing process costs, including different molds for each design, can be exorbitant. In addition, once an imperfection in the design is encountered, making design modifications on the full scale UAV prototype is difficult and expensive. Therefore, a cheap, rapid, and easily reproducible prototyping methodology is essential. Towards this goal, in this paper, we present such a low-cost prototyping methodology. The specific methodology starts with the manufacturing process of the foam core body production in a Computer Numerical Control (CNC) counter. Later, the vehicle frame is embedded in the foam core through aluminum profiles. After surface sanding and cleaning process, the body foam with an aluminum vehicle frame is coated with epoxy resin and fiberglass composite materials. In addition, various special design components such as landing gears, tilt mechanisms were printed using a 3D printer. Through this methodology, numerous 1/2 and 1/3 scale TURAC prototypes are built as the scale prototypes were sufficient in representing the dynamic behavior of the original system and at the same time giving us the flexibility to use commercial off-the-shelf (COTS) products in the power subsystem. These prototypes are used for refining not only the design through flight testing, but also for refining the flight controls systems for hover, forward flight and transition flight. The tests on the ground included thrust, structural, mechanism, and command-check tests. The flight tests involved conventional takeoff and landing, vertical takeoff and landing, and autonomous and transition flights.

The rest of the paper is organized as follows; in Section 2 we review the TURAC's design process, final design and the performance characteristics. In Section 3, a low-cost prototyping approach is introduced. Section 3 also includes a detailed account of the integration of the subsystems in the ready-to-test TURAC prototype. In Section 4, the general architecture of the ground station and the avionics system is reviewed. In Section 5, we present the tests cases and the results associated both ground and flight tests.

2 Design of the TURAC

The TURAC system has original design features such as a blended-wing multi-copter hybrid design for superior performance. The system includes several major innovations that overcome VTOL challenges like thrust vectoring, transition flight, and mechanical transformation from VTOL to Conventional Take-off and Landing (CTOL) flight. A series of analyses and tests of the systems and subsystems verify the design.

Computer-aided fluid, structure, and stability analyses were used to lower the development cost, but tests are indispensable for the aircraft development stage to confirm the analyses and design. System tests are one of the most critical stages of the TURAC design process.

Design studies start with understanding customer needs and design requirements, as shown in Fig. 2. Then configuration designs are made. Aerodynamic and structural analysis results are main inputs for detailing and enhancing the design. Wind-tunnel tests and flight tests are two of the most important inputs for aircraft design process. However, wind-tunnel testing couldn't be applied in this project because of the malfunctioned balance system. For this reason, CFD analysis and flight tests were used to understand aircraft stability and performance. Without wind tunnel inputs, most of the first flight tests are resulted in damage. Therefore, rapid and low cost prototyping methods are needed to obtain enough prototypes for flight tests.

2.1 Configuration and Sizing

The TURAC is based on a hybrid design that combines the hover flight capability of helicopters and the efficiency of conventional aircraft. It has a blended-wing airframe with a coaxial main lift fan and a two-tilt-rotor electrical propulsion system. The aerodynamic efficiency of the system is enhanced by up to 20 % with a blended-wing design in comparison to conventional fixed wing aircraft design [9]. Structure design is also less complex according to conventional aircrafts [10]. a Therefore, the system does not require a runway or a complex launch system for take-off and landing. It has superior endurance for performing surveillance and mapping missions. Moreover, the TURAC system uses an electrical propulsion system, provides the aircraft with silent and efficient flight. The system configuration is:

- Blended-wing multi-copter hybrid design,
- Two tilt rotors and one main coaxial lifting fan for VTOL operations,
- Winglet rudder hybrid design to reduce the structural weight and enhance aerodynamic efficiency,
- Electrical propulsion system for silent operations and superior propulsion efficiency,
- Tricycle retractable landing gear configuration for maximum ground control and reduced drag,
- Main lift fan doors for reduced drag,
- Redundant power and control system for safer civilian operations,
- High-capacity rechargeable lithium polymer power pack for extended endurance,
- Modular payload bay design for different types of missions,
- Detachable wings for easy transport and variable size wings for different operation requirements.

TURAC's VTOL capability is coming from its specialized electric propulsion system which is composed of two tilt-rotors and one main lift fan. Tilt-rotors are using at both of the flight regimes, VTOL, transition and forward flight. On the other hand, main lift fan is using only at the VTOL and transition flight. When front propellers are tilted vertical and main lift fan is used, system configuration is turned into multi-copter system. When main lift-fan is closed and tilt-rotors are positioned horizontally, system is turned into a blended-wing fixed wing aircraft.

Each of the tilt rotors have single brushless motor and propeller which are counter rotating to eliminate torque force. Main lift fan has two coaxial propellers with counter rotating turn and each of the propellers are driven by the independent motor-ESC units. When

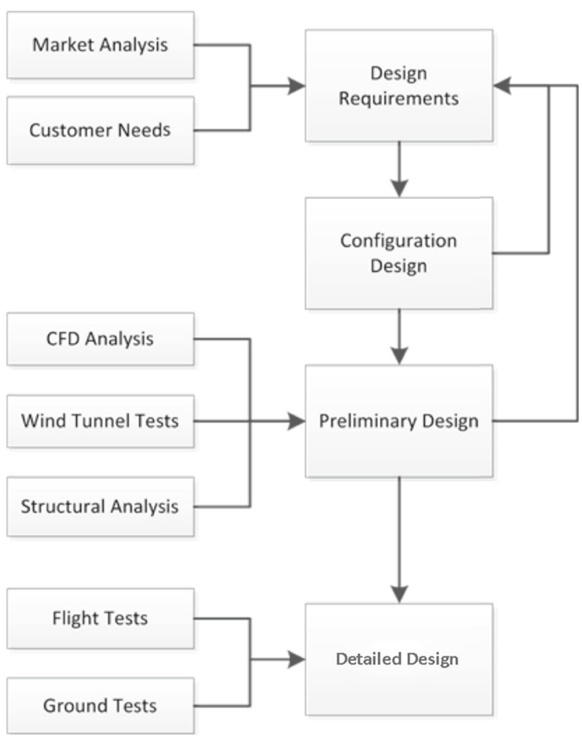

Fig. 2 TURAC design process

flying at hover or VTOL mode, yaw maneuvers could be done with changing the rotational speeds of propellers which are used in main lift-fan. Additionally, power storage is one of the most challenging part of the electric propulsion systems. In TURAC system, we use multiple packs of high energy density Lithium Polymer (LiPo) batteries with battery management system. This system controls all of the battery cells to use batteries more efficient and durable when discharging and recharging states.

Five versions of the TURAC have been prototyped and tested to enhance system reliability and performance (Table 1). Each version was tested for performance requirements to TURAC's performance goals, which was specified in the VTOL UAV competitor analysis (Table 1). The first version (V1) was designed with simple hand calculations and design loops in order to show the blended wing design and the capabilities of the TURAC team. Aerodynamic Vortex Lattice Method (VLM) code was developed and integrated empirical calculations with design cycles until V2. For V3, stability was the key issue and most of the work to enhance stability aerodynamic efficiency. High-level aerodynamic and structural analyses were applied to finalize the design. Flight tests were used to understand the system and behaviors of V4. Most of the subsystems were developed and tested for the V4 platform and subsystems like the tilt mechanism and main lift fan were finalized. V5 is the final version and most of the test flights were done with it, in addition to aerodynamic, structural, and propulsion optimization studies. Stability enhancement studies were finalized with V5 after successful forward flight tests. Transition flight tests were continued and successful transition maneuvers were done with the 1/3-scale prototype.

Based on studies and flight test of V5, improvements were made to the airfoil, center fuselage geometry (for high volume payload), and main lift fan. These modifications improved performance and stability of the aerial platform. The final design is tabulated as Table 2.

Proper weight estimation is essential for achieving the targeted performance value of an aircraft. For this reason, component-based weight estimation and distribution studies were done to calculate maximum take-off weight (MTOW). Battery weight is the most significant component and can reach 60 % of

Table 1 TURAC versions and development purposes

	TURAC V1 Conceptual design Basic design calculations Concept proof prototyping and flight test
	TURAC V2 Preliminary aerodynamic design stage calculations Design update for hybrid propulsion Mechanism designs
	TURAC V3 Optimization for electric propulsion Stability enhancement Applying custom prototyping methods
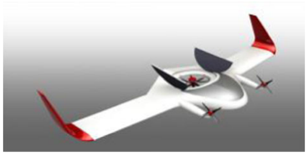	TURAC V4 Detailed design CFD and structural analysis Structural and mechanical tests VTOL subsystem development
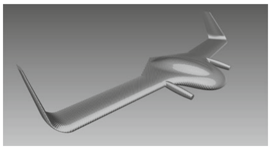	TURAC V5 Aerodynamic, structural and systems optimization VTOL and CTOL tests Transition flight tests

Table 2 TURAC final sizing results

TURAC V5 SIZING RESULTS		
WEIGHT DISTRIBUTION	Payload	8 kg
	Structure	10 kg
	Avionics	2 kg
	Battery	20 kg
	Propulsion	7 kg
	Maximum Take-off Weight (MTOW)	47 kg
DIMENSIONS	Length	1.8 m
	Wingspan	5.2 m
	Height	1.25 m
	Wing Area	3.825 m^2
	Aspect Ratio	8.28
	Mean Chord	0.91 m
	Propeller Diameter	0.43 m
	Aerodynamic Center* (AC)	0.8355 m
	Center of Gravity* (CG)	0.790 m
*Distance from the center chord's leading edge		
FUSELAGE	Center Airfoil	MH92
	Tip Airfoil	MH78
	Fuselage Length	1.8 m
	Fuselage Span	1.6 m
	Center Chord	1.8 m
	Tip Chord	0.58 m
	Taper Ratio	0.322
WING**	Root Airfoil	MH78
	Tip Airfoil	MH92
	Chord	0.58 m
	Span	1.6 m
	Swept (LE)	10°
	Anhedral	5°
	Elevon Length	1.6 m
	Elevon Width	0.145 m
WINGLET	Airfoil	NACA 04012
	Area	0.313 m2
	Length	0.634 m
	Swept (LE)	38°
	Root Chord	0.6 m
	Tip Chord	0.278 m
	Aspect Ratio	1.5
	Taper Ratio	0.397
	Rudder Length	0.5 m
	Rudder Tip Width	0.07 m
	Rudder Root Width	0.15 m

Table 2 (continued)

**Wing consists of two detachable parts, results for each part.		
LANDING GEAR*	Height	0.421 m
	Front LG Distance	0.4 m
	Main LG Distance	0.897 m

*Distance from the center chord's leading edge

the MTOW in electric propulsion [11]. Computational Fluid Dynamics (CFD) analyses were used to find the required thrust and power levels and the propulsion system was updated over the design cycle. After an iterative selection process, power consumption and battery weight could be calculated for targeted performance values. On the other hand, a sizing study was done with the same design iteration. Weight estimation and aircraft performance needs were the two main factors for general sizing. Moving surface sizing was optimized with stability requirements and the CFD analysis. Further information about weight estimation and sizing process can be found in [1].

The TURAC V5 is the final design. A Computer-Aided Design (CAD) drawing of the aircraft is shown in Fig. 3, and 4. The blended-wing design allowed us to make efficient flights with minimum structural weight [10]. Carbon fiber and other composite materials were used for a lighter structure, in addition to a winglet-rudder hybrid design. This also reduces drag generated from the wing tip vortices and sustains stability around the vertical axis. The TURAC system has four independently controlled electric motors. Two were designed with the tilt mechanism to be used in forward, transition, and vertical flight regimes. The other two are used by the main lifting fan for vertical and transition flight. This fan has counter-rotating propellers with two independently controlled brushless motors. Changing the rotation speed of the main lift fan propellers causes a difference in torque equilibrium that can used to make yaw maneuvers.

Inboard design was an important issue for payload integration and setting the CG location after integrating different payloads. The battery accounts for most of the system weight and is located next to the main lift fan. Avionics had to be located at the CG of the aircraft to meet control requirements. A modular payload

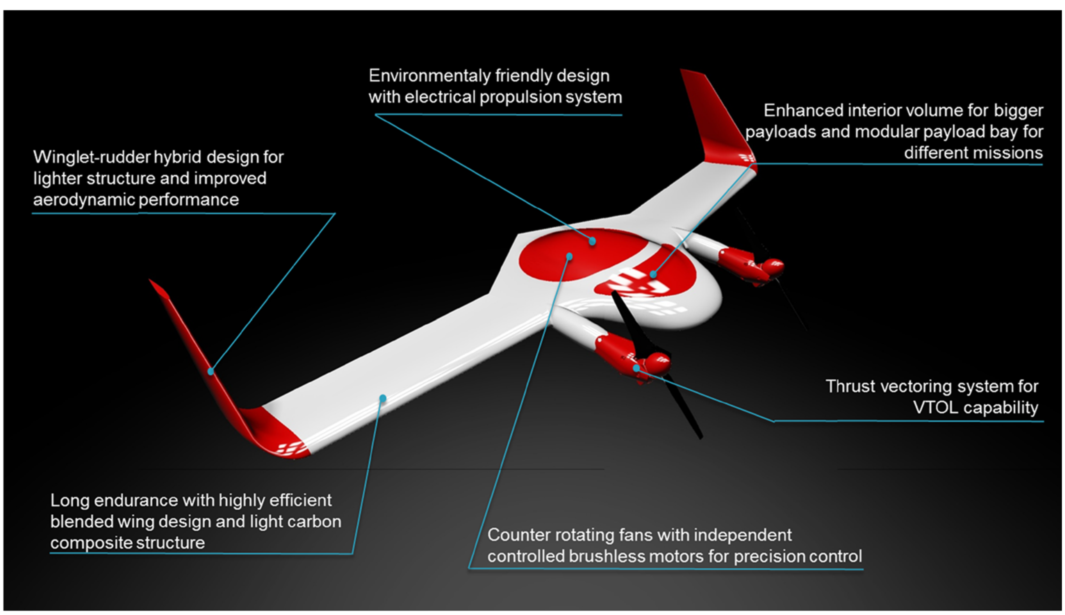

Fig. 3 TURAC UAV design features

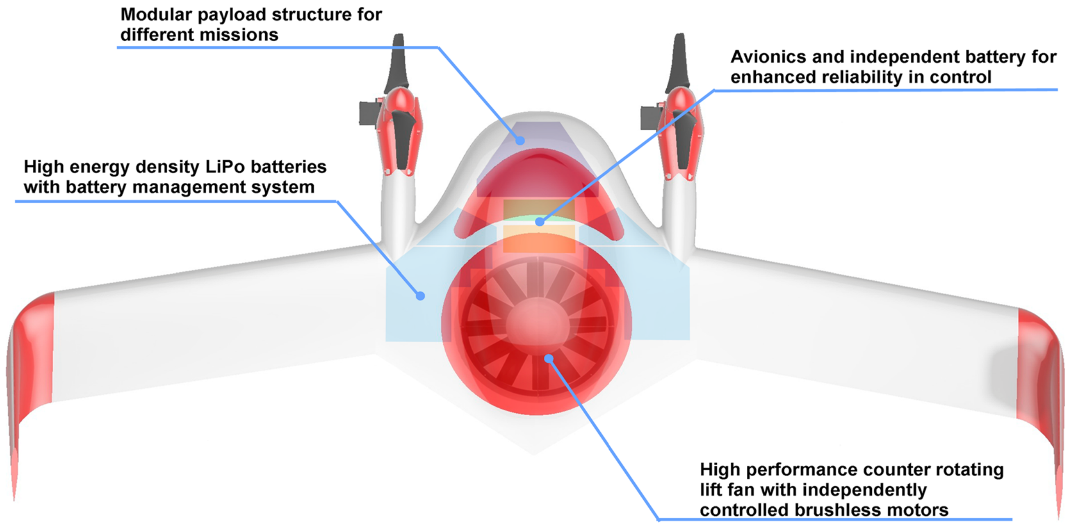

Fig. 4 TURAC inboard design

bay was located at the front of the aircraft for easy CG integration and setting.

In the next section we focus on the two key modeling and analysis aspects of the TURAC, the aerodynamic and structural aspects, which both played a key role in the manufacturing process.

2.2 Aerodynamic and Structural Analysis of the TURAC

This section investigates aerodynamic and structural analyses, which are fundamental for aircraft design. Following empirical approaches and sizing studies of earlier prototypes, aerodynamic analyses were used to enhance performance and stability. Structural analyses were done to reduce weight and increase structural reliability. Ultimately, the final sizing is determined by these comprehensive analyses.

Aerodynamic calculations were separated into mathematical models and CFD analysis, which is detailed in [4, 12]. CFD analyses were applied to determine the variability of aerodynamic coefficients at different forward flight velocities with different angles of attack. For the specific analysis, Fluent was used as the solver and K-epsilon Enhanced Wall Treatment turbulence model was used. Figure 5 shows such an analysis in which the streamlines in forward flight was identified. Such streamlines played a key role in understanding the effect aerodynamic configuration changes on the flow around the lifting fan.

For transition flight, various scenarios across a wide range of tilt propeller angles, angle of attacks and forward speeds were analyzed. In these analyses, tilt and coaxial propellers were defined via fan boundary conditions with pressure jumps. As such, the velocity contours of the coaxial fan are shown in Fig. 6. Specifically, velocity is noted to be higher behind the upper propeller of the coaxial fan than in front of it. These analyses indicate that airflow during transition is very complex. We again refer the reader to [4, 12] for an extensive treatment of not only the aerodynamic analysis but also the intertied dynamic modeling aspect.

For structural analysis, modeling was carried out mostly with finite element methodologies which used the composite materials that were utilized during design. In the structural analysis, CFD identified pressure loads were integrated into the structure with the FLUENT program. Engine thrust and loads due to gravity were also included in the analysis. Static analyses were conducted with positive and negative limit load scenarios. As a result of these analyses, maximum displacements, maximum stress, and strain values were calculated under load-limit scenarios. Based on load limits, structure failure theories were explored. Stress distributions and failure indices were checked

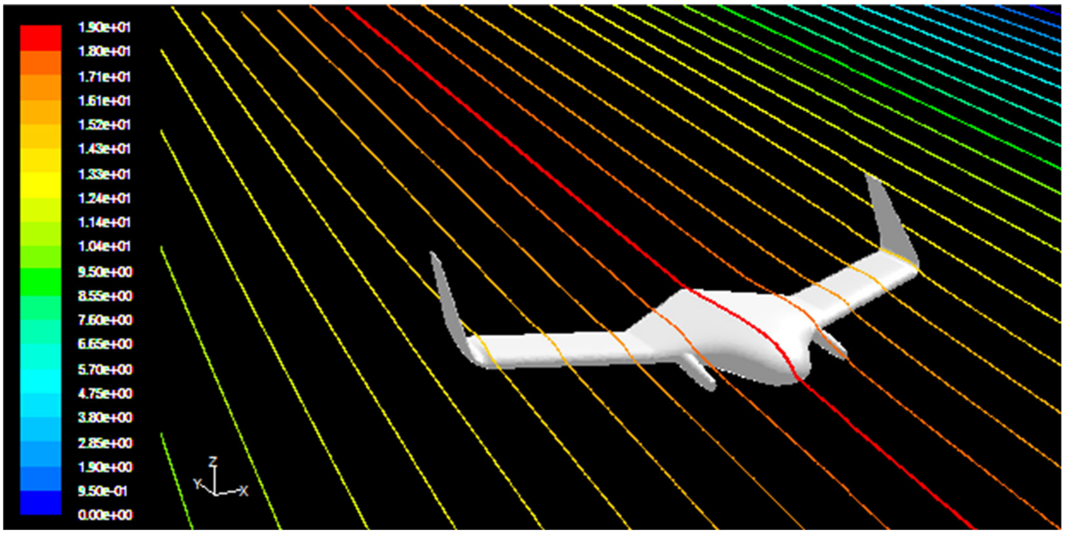

Fig. 5 CFD analysis the TURAC at forward flight showing streamlines

and then the structure was optimized as shown in Fig. 7. To reduce failure risk, the places with high failure indices were strengthened with extra layers of carbon and fiberglass composites during the manufacturing process.

Connecting joints for the detachable wing and tilt mechanism are naturally under high loads and are also failure risks (as shown in Fig. 7).

The TURAC has several mechanical subsystems such as tilt mechanisms, landing gears, and main lift fan doors. Subsystems' structures were analyzed with finite element methods to find possible failure scenarios. For example, tilt mechanism bending or deflection can cause the propeller to crash with the tilt mechanism booms. Therefore, tilt mechanism deformation analysis was done to find deflection under maximum load. If the deflection ratio was outside of acceptable limits, the structure was redesigned. Figure 8 shows the deflection of the tilt mechanism under maximum MTOW load and thrust condition. [13]

2.3 Performance

This section presents performance calculations of the final TURAC design The propulsion system is the

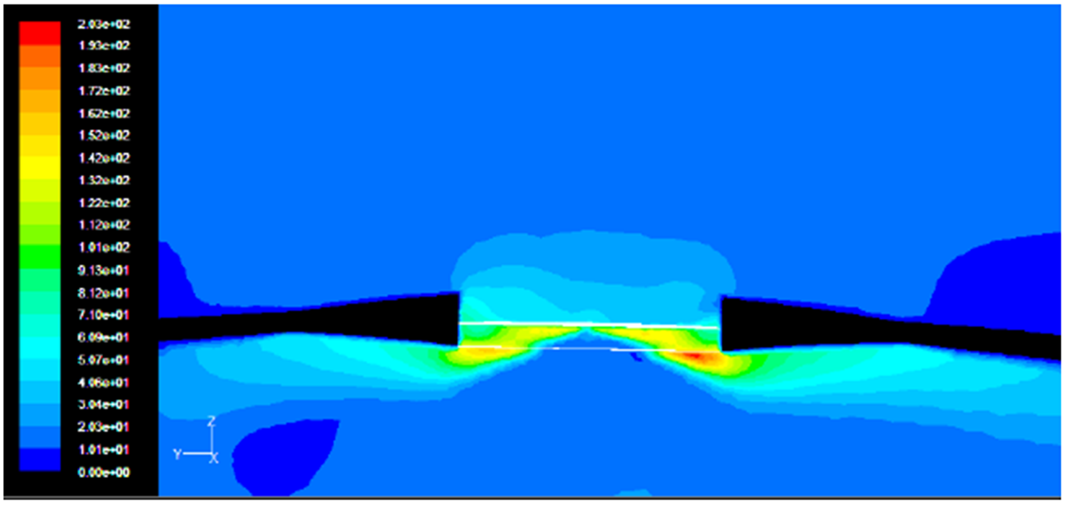

Fig. 6 Velocity contours of the coaxial fan

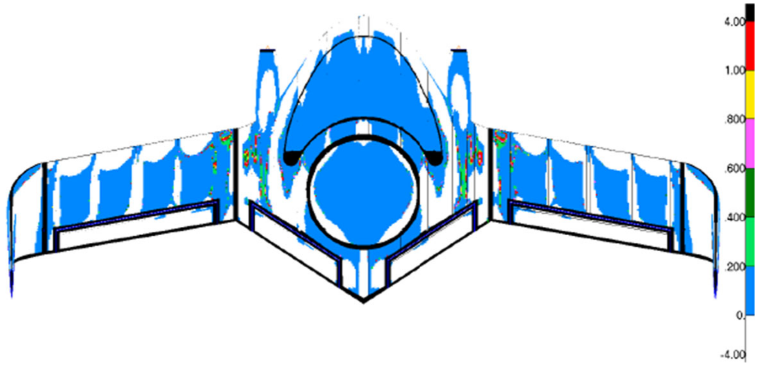

Fig. 7 Failure-index distributions under positive load limits

LiPobased electric propulsion system, which has more than 60 % efficiency [11] In addition the hover-optimized main lift fan with coaxial rotors and duct case dramatically increase hover time as compared to conventional rotor systems [14]

The TURAC is primarily planned to be used for civilian surveillance and mapping missions that require long endurance. For this reason, the minimum power flight velocities were calculated for flights of long endurance and range. The maximum rate of climb was an important parameter for mission planning and power management. The maximum glide range was calculated for emergency situations such as propulsion system malfunction.

Figure 9 shows the performance calculation method. CFD results were used at the preliminary design stage in order to refine the design. The aerial platform was modeled and analyzed with Fluent CFD software with different speed and angle of attack conditions. Maximum L/D ratio is approximately 5° angle of attack, which allows the aircraft to fly in the most aerodynamically efficient flight regime. This condition is also used for trimmed flight.

Thrust tests provided another important input for performance calculations. Seven brushless electric motors and 14 propellers were analyzed and tested on the thrust test bench, which was developed specially for this project.

Excess power and thrust is essential for a high climb rate and tight turns in conventional flight, but for a VTOL like the TURAC, they are needed during hover and transition flight. The complete set of TURAC key performance calculations results are shown in Figs. 10, 11, 12, and Table 3.

The stall speed of the TURAC in conventional flight is 17 m/s. Required thrust was calculated from the C_D values, which come directly from CFD

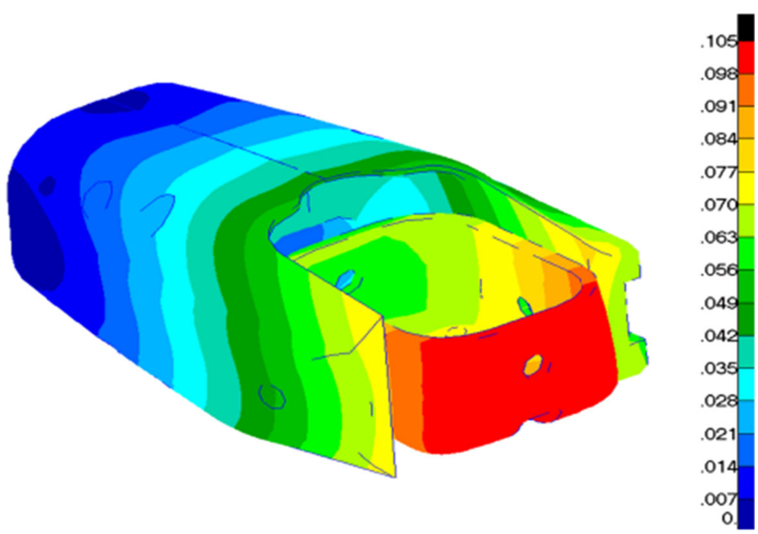

Fig. 8 Tilt mechanism deformation distributions (mm)

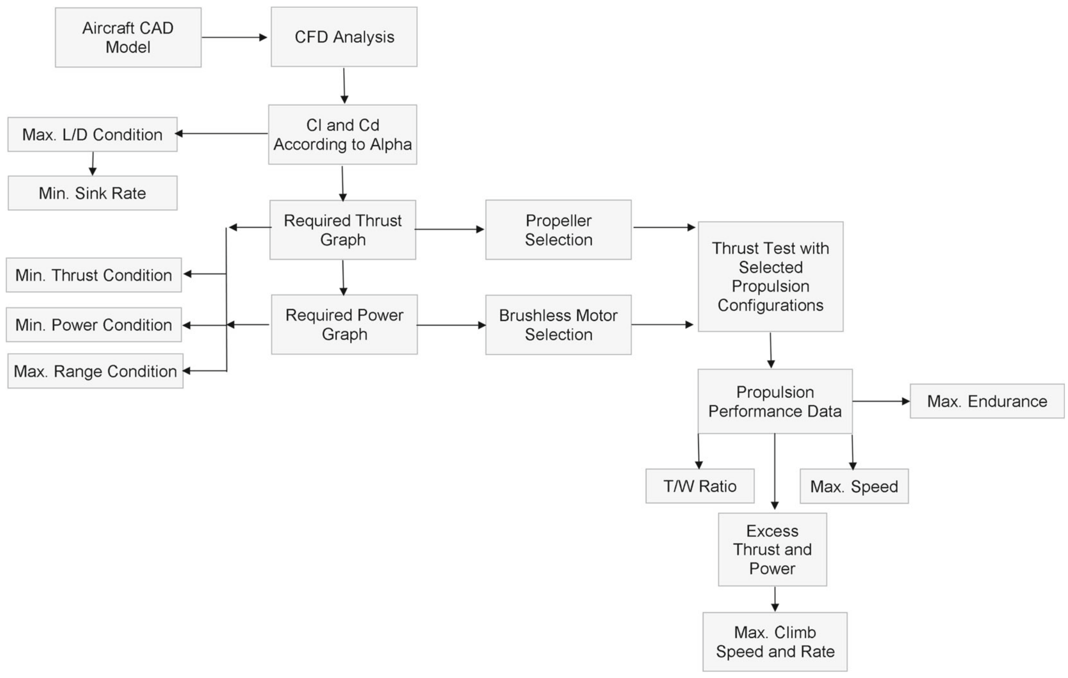

Fig. 9 Performance calculations according to CFD results and thrust tests

analysis. At constant speed, drag equals the thrust so it is simple to identify required thrust levels for designing the propulsion system. In Fig. 10, blue lines shows the required thrust levels and red line shows the available thrust, which is used to design of the propulsion system's thrust capacity. An intersection between required and available thrust shows the maximum speed of 49 m/s.

Figure 11 shows the TURAC's required and available power levels, which were calculated the same way as thrust. For required power, the minimum speed after stall speed is the most important for UAVs, because it shows the minimum required power to fly. This also indicates minimum power consumption from a restricted battery capacity and maximum flight time. The minimum required power at 20 m/s allows for maximum endurance. A tangent from the origin to the required power shows the most efficient flight regime, which is the same condition with maximum L/D and at 25 m/s.

Fig. 10 Thrust required and thrust available for conventional flight

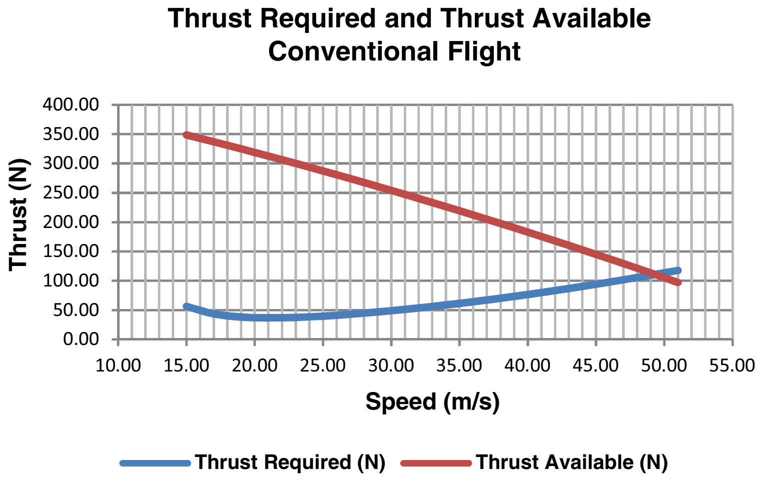

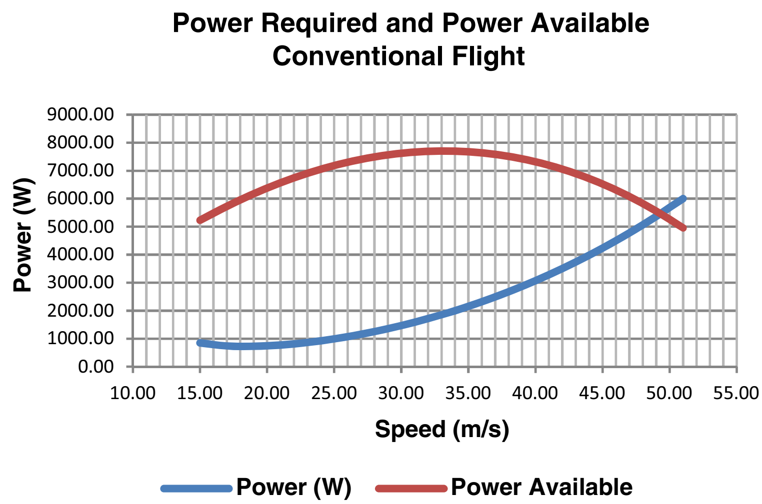

Fig. 11 Power required and power available conventional flight

Excess thrust and power versus flight speed was calculated to evaluate climb and maneuver performance. These values were used to calculate maximum climb angle, climb rate, and turn radius. The principal performance parameters of the TURAC system are in Table 3.

These parameters were used to further enhance TURAC's autopilot, power management system, and overall performance. Further refinements were based on flight tests with scale prototypes, which are detailed in the following section.

3 Prototyping the TURAC

During the design process, flight testing was key in understanding the effect of various design features towards the performance and stability of TURAC. For this reason, prototyping became one of the most important issues in TURAC's development. All aerodynamic, structure, and system tests were applied on semi- or fully-functional prototypes. In that sense, the prototyping process needed to be rapid and low cost in order to meet the project schedule and budget. At the same time, each prototype must be conform to the design and be durable enough to make several tests. For this reason, existing methods were improved with new methods such as 3D printing.

Figure 13 show TURAC 1/3-scale prototype expanded view and materials. Here composite parts were used as the main structure and most of the precision parts like mechanisms and connections were from 3D printing.

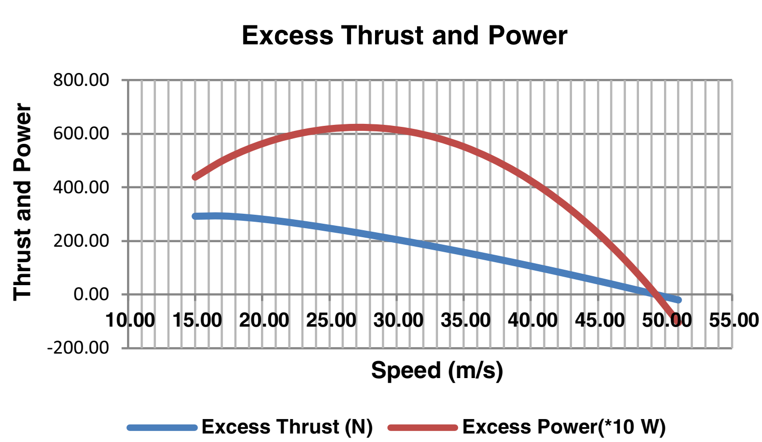

Fig. 12 Excess thrust and power

Table 3 Principal performance parameters for TURAC UAV

PERFORMANCE RESULTS			
Mission Profile		Thrust Distribution	
Starting Altitude	Sea Level	1. Tilt Thruster	15%
Mission Altitude	1000 masl	2. Tilt Thruster	15%
Max Altitude	4500 masl	Main Thruster	70%
Endurance			
VTOL	CTOL		
Flight Mode	Time (min)	Flight Mode	Time (min)
VTOL	10	VTOL	none
Climb	7.5	Climb	7.5
Cruise	60	Cruise	180
Descent	7.5	Descent	7.5
TOTAL	85	TOTAL	195
Speed (m/s)			
Range ($V_{\mathbf{cruise}}$)	25	**Max L/D**	12.47
Endurance ($V_{\mathbf{loiter}}$)	20	Max. Climb Angle	32°
Max ($V_{\mathbf{max}}$)	49	Max. Climb Rate	1355 m/s
Stall ($V_{\mathbf{stall}}$)	17	Min. Sink Rate	1686 m/s

3.1 A Low-Cost Manufacturing Approach

A low-cost, rapid, and reproducible manufacturing approach was used for TURAC development. The 1/2- and 1/3-scale models provided enough dynamic similarity to the full scale system and were easier to operate and manage. Full scaled prototype will be produced after finalizing scaled prototype tests. In

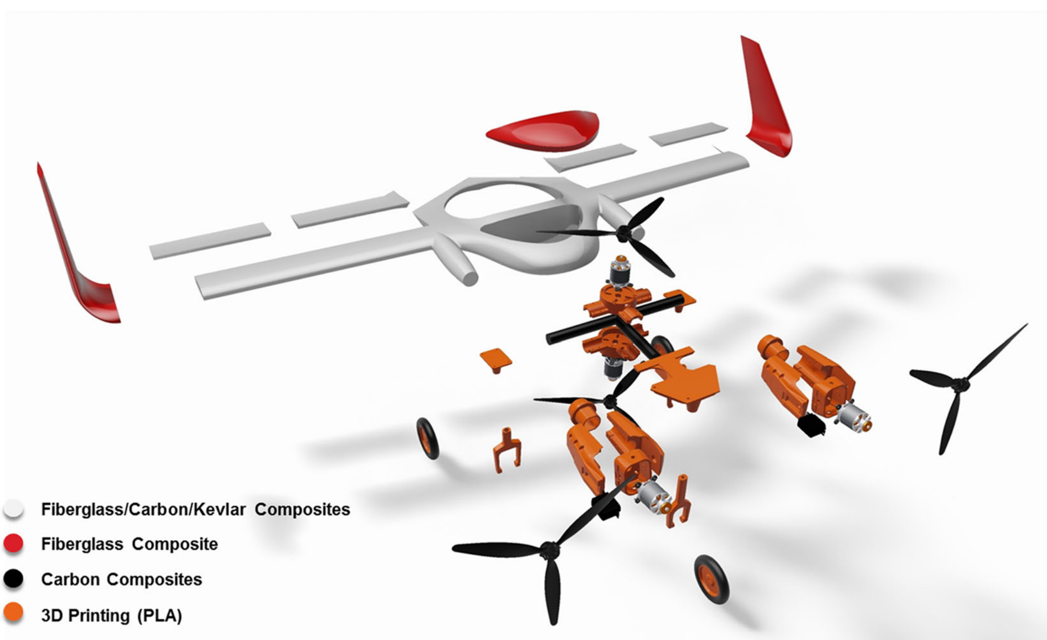

Fig. 13 TURAC 1/3-scale prototype expanded view of parts and associated materials

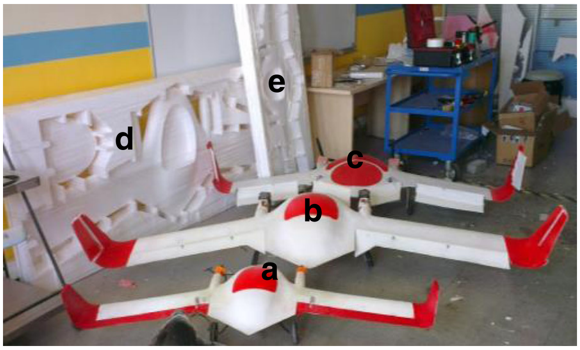

Fig. 14 **a**) $1/3$-scale for forward flight **b**) $1/2$-scale for forward flight **c**) $1/2$-scale VTOL **d**) 1/2-scale for forward flight **e**) $1/3$-scale for forward flight

addition, Scaled models allow the project team to use standard parts such as propellers, ESC, and brushless motors that can be easily found at local hobby stores. Prototype production utilized COTS parts as much as possible to reduce time, energy, and cost. This is different from the original TURAC system, which has numerous custom parts such as the landing gear and door mechanisms. In total, fifteen prototypes were made for flight testing and two of them for transition tests. Figure 14 shows examples of three finished and used prototypes and two foam core structures.

During the production phase, different production methods were evaluated for TURAC prototypes (Table 4). Specifically, Composites are very lightweight and can be produce with precision, but during design, prototypes need to be changed after test flights so many molds are required. The prepreg method is very effective way to build a composite structure, but needs additional production infrastructure like autoclave and high-quality, temperature resistant molds. Given their high costs, no molds were used in prototyping. Hand lay up composites with CNC machined foam core was selected for TURAC prototyping because of its low cost and easy manufacturing [15–17]. Machine shop and CNC production at university facilities was preferred. Simple internal design was done to reduce production time.

A durable prototype design and manufacturing process were required to make several tests on one prototype. A foam-core fiberglass composite method also provided good surface quality and enough durability in test flights [15].

3.2 Manufacturing Process

CAD was used in the design process. All technical drawings were done with CAD software and the manufacturing process was based on CAD outputs. The manufacturing process of a $1/2$-scaled prototype is shown in Fig. 15 and the prototyping sequence as photographed step-by-step in Fig. 16.

Aluminum profiles are formed and cut with hand tools according to the CAD drawings. While the aluminum structure was being manufactured, the foam core was formed with a CNC machine to reduce the production time. Next, the two components were

Table 4 TURAC comparative prototyping method selection [15, 16]

TURAC Main Structure Prototyping Methods	Cost	Ease of Manufacturing	Precision	Durability	TOTAL SCORE
Parameter Weight	40	30	10	20	100
CNC Machined Mold, Hand Lay Up Composites	2	4	4	4	320
CNC Machined Mold, Prepreg Composites	1	3	5	5	280
Male-Female Composite Mold, Hand Lay Up Composites	4	2	3	3	310
CNC Machined Foam Core, Hand Lay Up Composite Wrapping	5	3	1	2	340

*Scored from 1 (worst) to 5 (best)

**Score weights are used to show the importance of prototyping in TURAC Project

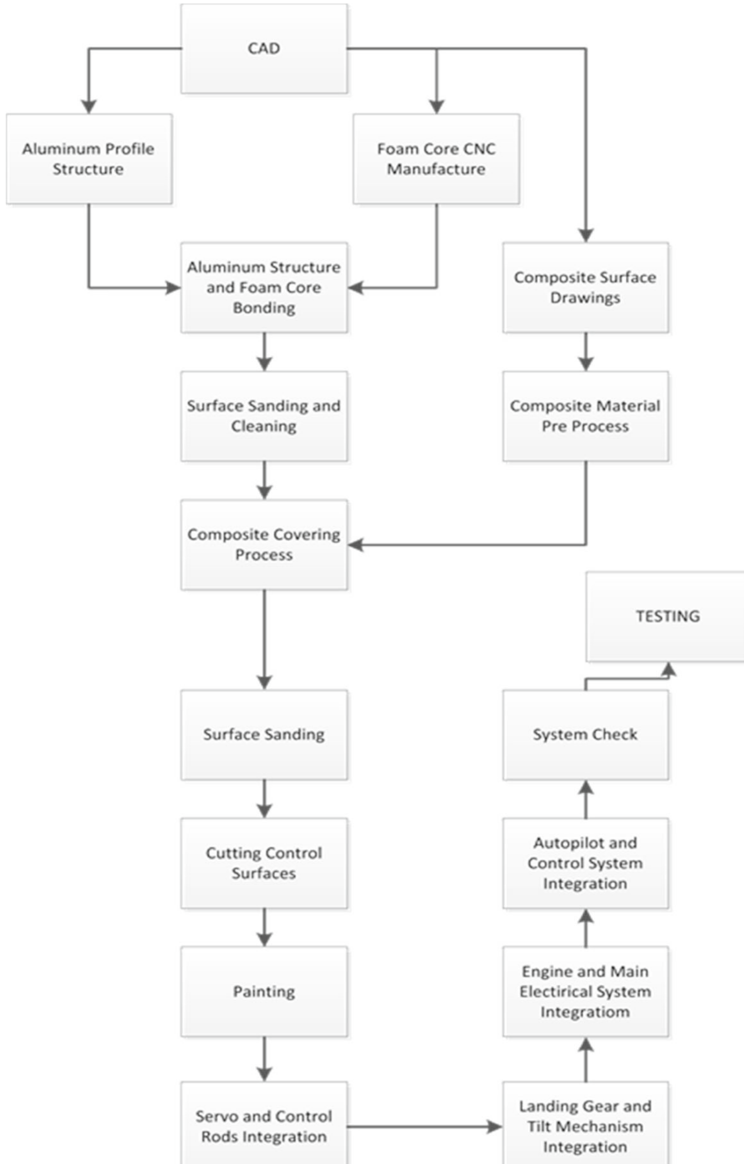

Fig. 15 1/2-scale TURAC prototype manufacturing process

glued together with foam adhesive, making the structure stiffer than one joined with bolts.

Next, surfaces were sanded and cleaned before composite coating. Composite materials are cut with scissors following CAD drawings. Epoxy resin and fiberglass composite materials were used to coating the foam core with aluminum. Control surfaces were cut with a high-speed metal disk. Then, hinges and control horns were integrated into the control surfaces. The surface was cleaned with pressurized air and a wet cloth. A few layers of paint were applied to make the surface smoother. Finally, the landing gear, mechanisms, propulsion units, and control system were integrated before a system check.

The TURAC team improved the manufacturing process after V1. After several hard landings, the aluminum structure had some problems like bending and disjointing from the foam core. Next, carbon tubes were used to manufacture a lighter and more reliable structure, but carbon tube joints caused disjointing and cracking. Finally, the team used foam cores, fiberglass, carbon fiber, and more flexible epoxy resin.

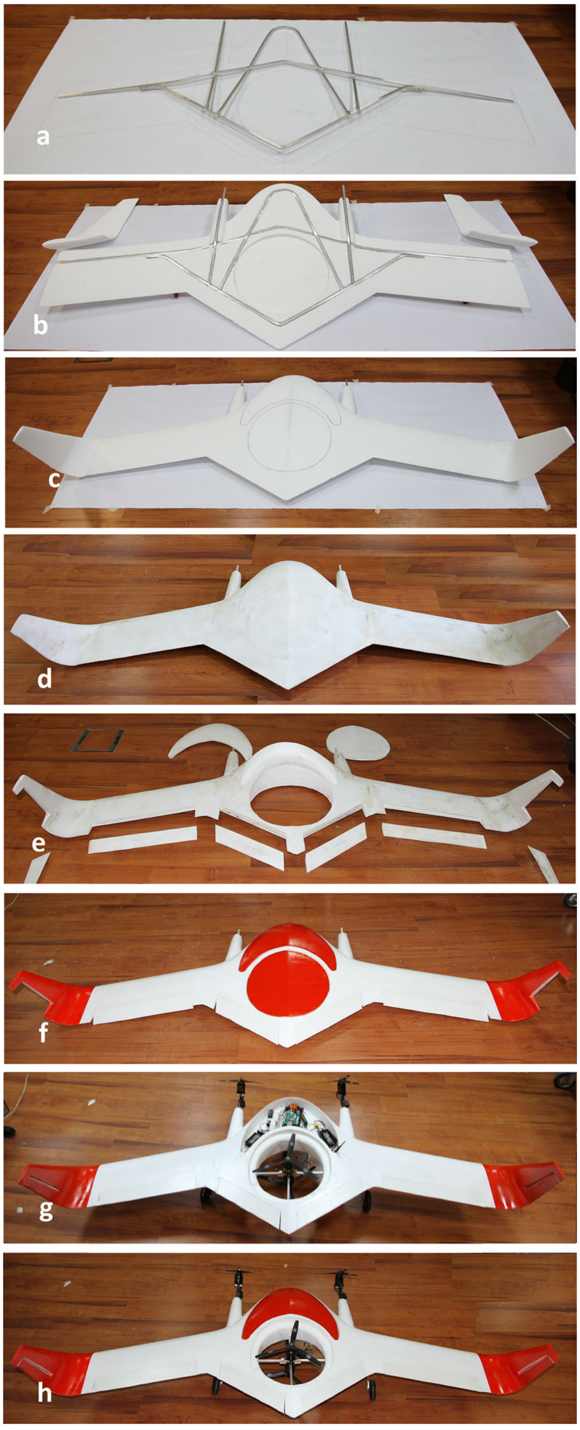

Fig. 16 **a** Aluminum structure production with technical drawings **b** Foam core CNC manufacturing **c** Aluminum structure and foam core bonding **d** Composite material covering and surface sanding **e** Cutting control surfaces **f** Painting **g** Systems integration **h** Systems check

After several tests and hard landings, the structure was found to be more reliable than previous versions and flexible enough to eliminate cracking after impact.

Removing the aluminum structure from prototype manufacturing makes the structure more reliable, reduces weight, and decreases manufacturing time significantly.

3D-printing systems make possible a rapid production of mechanisms and precision structures like servo connections and motor mounts. Different rapid prototyping techniques in the 3D printing market as shown in Table 5, but Fused Deposition Modelling (FDM) technique in Fig. 17 is selected for its advantages like low cost solution, accessible from local market and offering wide variety of materials [18, 19]. FDM technology gives rough surfaces but mechanical treatment could be applied to make fine surfaces. Print like honeycomb composite geometry to have rigid and light structures which is shown in Fig. 18 is another advantage of FDM technology.

Figure 19 shows the 3D-printing system printing the 1/3-scale prototype's tilt mechanism using FDM technology. The system uses a biodegradable plastic material PLA (Polylactic Acid) filament and an extruder melts the filament and moves over the print table with CNC G-codes.

Previously, complex geometries could not be easily manufactured with this technology. Design boundaries and time limits have changed with this technology. Thanks to the 3D-printing system, the TURAC team had design freedom and innovative solutions could be developed rapidly. Figure 19 shows the new design philosophy for manufacturing tilt mechanisms.

Conventional manufacturing methods and materials and 3D-printing technology are compared in Table 6 for the 1/2- scale prototype tilt mechanism. For most of the parameters, conventional methods require more than one production method to manufacture one set of tilt mechanisms because of the limited production of different geometries and materials. Craftsmanship needs to be specialized in order to use different production techniques like CNC machining, laser cutting, and bending. Different production techniques also require more time and are costlier than 3D printing. As a result, 3D printing has become the method of choice.

In next section, the avionics systems and the flight control system is detailed. The flight control system

Table 5 3D printing technology comparison [18, 19]

Technology	Material	Cost 1–10	Surface Quality	Durability
Streolithography (SLA)	Liquid Resin	8	Fine	Low
Fused Deposition Modelling (FDM)	ABS, PLA, PET	2	Rough	Medium
Multi-Jet Modeling (MJM)	Liquid ABS	10	Fine	High
Selective Laser Sintering (SLS)	Powder ABS, Kestamid	7	Medium	High
Laminated Object Manufacturing (LOM)	Adhessive and paper	5	Medium	Low

has been instrumental in enabling stable and fully controlled VTOL and CTOL flights.

4 Avionic System and Ground Station

TURAC has a unique control system for making CTOL, VTOL, and transition flights. In the next subsections, we review the key aspects associated with the flight control system.

4.1 Avionic System

The general architecture of the system is shown in Fig. 20. The entire system can be divided into the ground station and avionics. The avionic system includes an autopilot, sensor packages, radio control receiver, telemetry modules, and actuators. The autopilot system includes a flight control computer and a flight management computer. The Flight control computer handles low-level control loops while the flight management computer executes the high-level navigation loops.

The flight control computer is based on a 32-Bit STM32F4 processor with a Cortex-M4 core, 168 MHz , 192 KB RAM, and 1 MB Flash Memory. The flight control computer is a custom board with an STM32 board so other units can be connected, as shown in Fig. 21. It handles low-level in-circuit communication as shown in Fig. 22. External peripheral units, such as the IMU/INS/GPS sensor kit, radio control receiver, actuators, data-logger, pitot tube, alpha and beta sensors, battery management sensors and, naturally, the flight management computer are connected to the flight control computer by serial or analog interfaces. Detailed information can be found in [8].

The Flight Control Computer deals with flight control loops and managing low level communications as mentioned above. Flight control loops can be seen in Fig. 22 for the hover state. Our IMU/INS sensor suite,

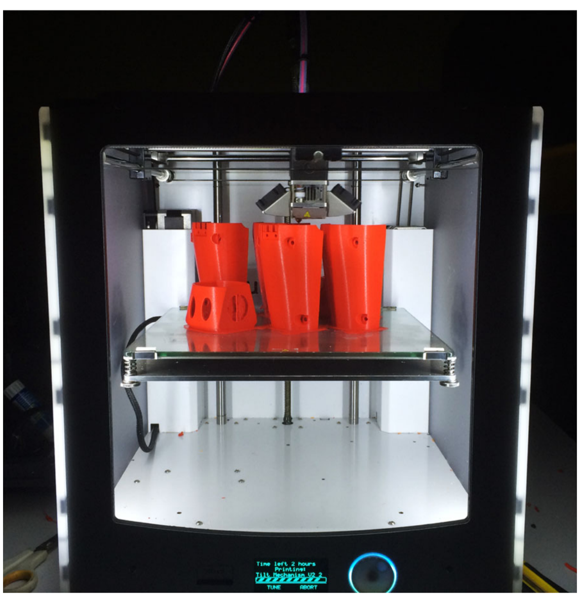

Fig. 17 3D printing of 1/3-scale prototype tilt mechanisms using Fused Deposition Modelling (FDM) technology

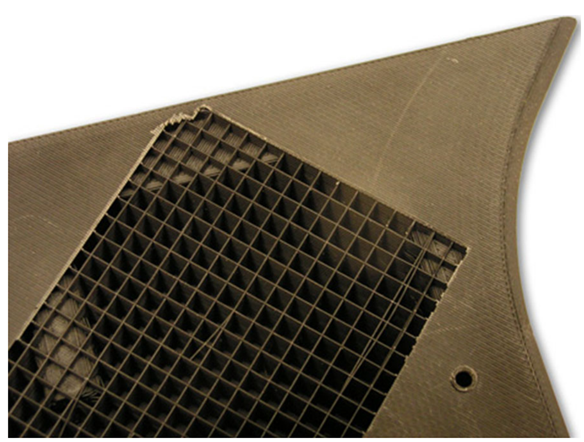

Fig. 18 Honeycomb composite like structure produced in FDM technology with ABS plastic material

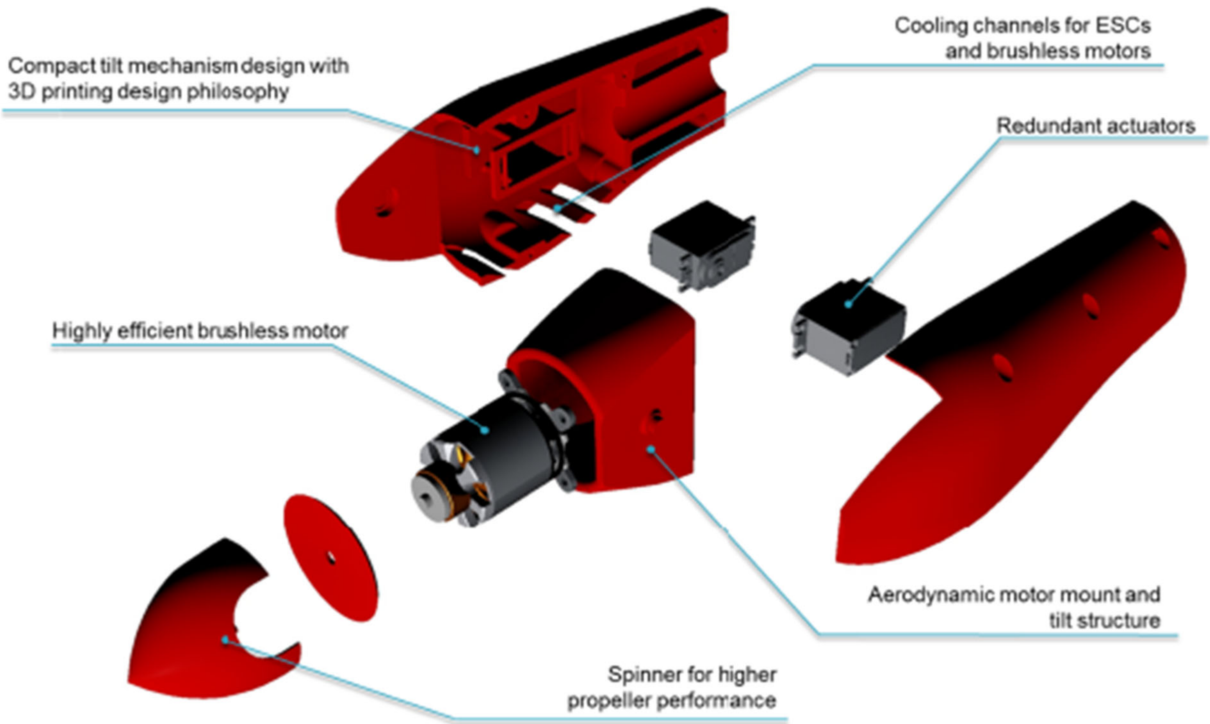

Fig. 19 Tilt mechanism design with 3D printing design philosophy

which is the MTI-G-700 from Xsense, outputs feedback values, such as position, velocity, orientation, and angular rates for controllers.

The Flight Management Computer (FMC) executes high-level navigation operations and also drives the flight control computer when auto-navigation is enabled. The Flight Management Computer is based on a Linux operating system and a single-board computer that runs at 720 MHz and is called "Raspberry Pi." The FMC is connected to the ground station with two options, a 2.4 GHz WiFi modem and a 900 MHz RF modems, which are complementary. The Wi-Fi modem has a short range but a very high data rate transfer, 54 Mbps in theory. The RF modem (900 MHz X-Tend by Digi) has a very long range but a low data rate transfer, about 115 Kbps in theory. Each one can be selected in flight depending on how far the aircraft is to fly.

In the next subsection, we focus on the ground control station, which is used to control inputs to the aircraft and receive telemetry and valuable data from payloads.

Table 6 Comparative evaluation of tilt mechanism production

Prototyping Process for Tilt Mechanisms		
	Conventional Methods	3D Printing
Material	Aluminum, Kestamid	PLA, ABS
Process	CNC, laser cutting, bending	Fused Deposition Method (FDM)
Weight	High (limited production methods)	Low (advanced geometry structure production)
Craftsmanship	Specialized skills, more than one craftsman	Few skills, one person is enough
Durability	Durable	Durable
Time	Long	Short
Cost	High (different manufacturer and materials)	Low (single material, wide range of suppliers)

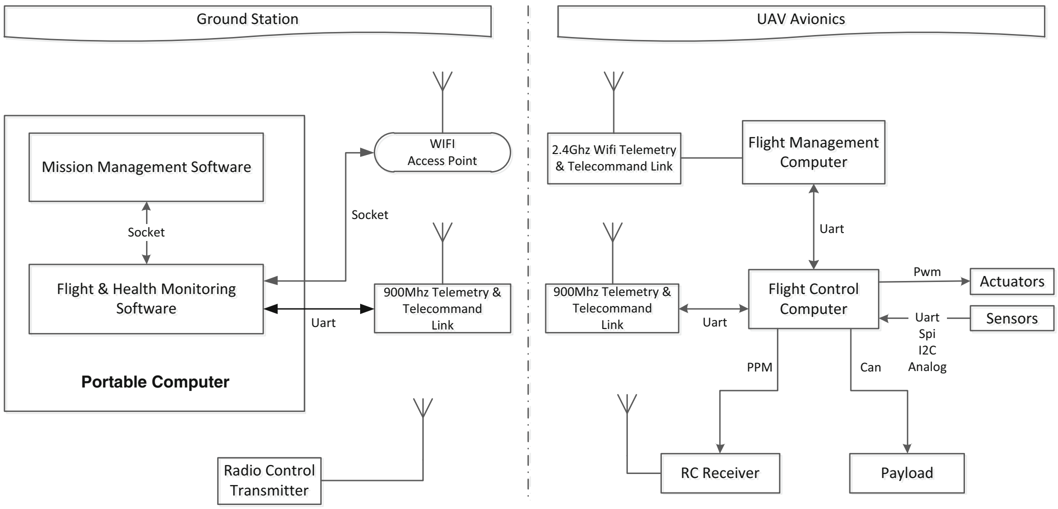

Fig. 20 Architecture of the Ground Station and Avionics

4.2 Ground Station

The Ground Station (GS) includes a radio control unit for manual flights, an RF modem, a Wi-Fi router and a computer that runs a Graphical User Interface (GUI), as shown in Fig. 25. The main communication link is established by a Wi-Fi connection but an RF modem is used as a backup, which is connected via USB.

Ground Station Software (GSS) was developed in C++ programming language, which is seen in Fig. 22. It allows for monitoring, configuring primary control parameters, and uploading fully autonomous mission steps. The main GUI consists of three sections as seen in Fig. 23. The upper left side is a heads-up-display with real-time video from the vehicle camera in the background. The heads-up-display include flight data such as orientation, coordinates, altitude, battery status, communication status, operator control inputs, vehicle mode and navigation status. The right side of the GUI is a map overlay. This overlay allows for tracking the vehicle and managing

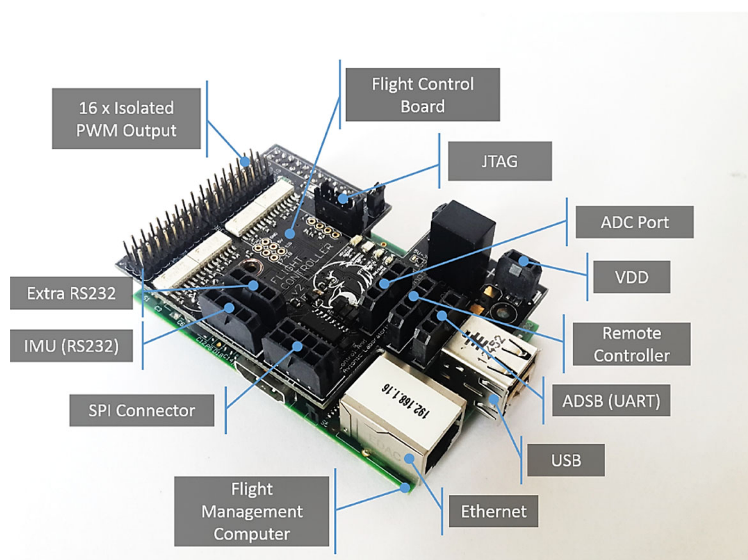

Fig. 21 The Flight Management Computer and Expansion Board

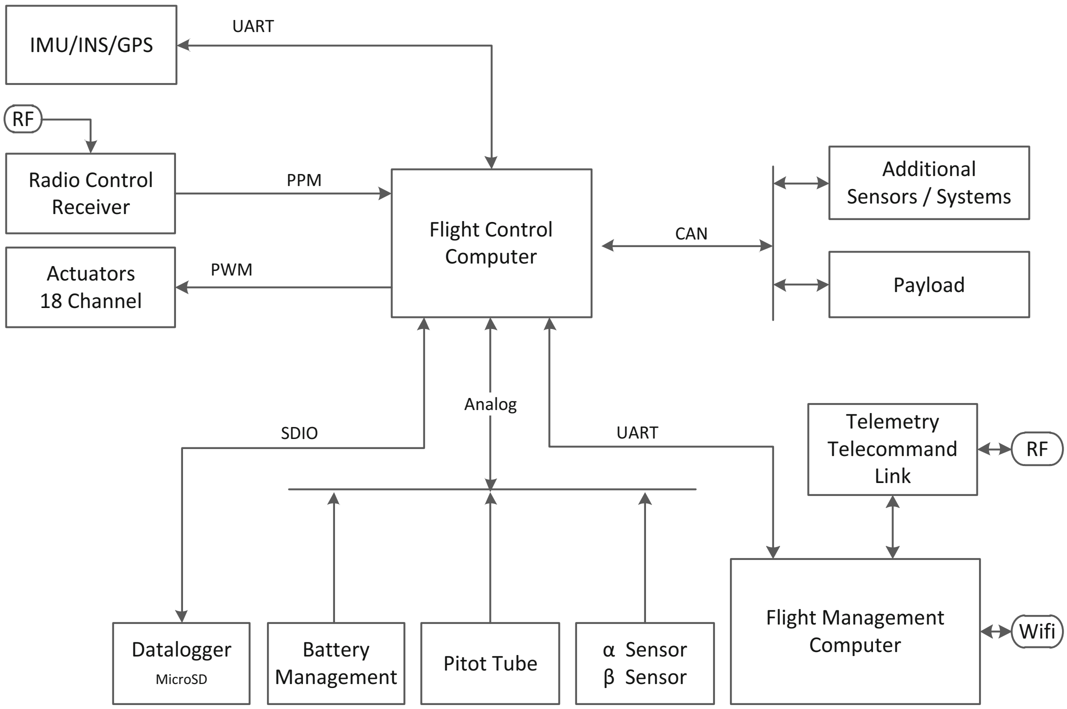

Fig. 22 Flight Control Computer and Its Peripherals

Fig. 23 Ground station graphical user interface

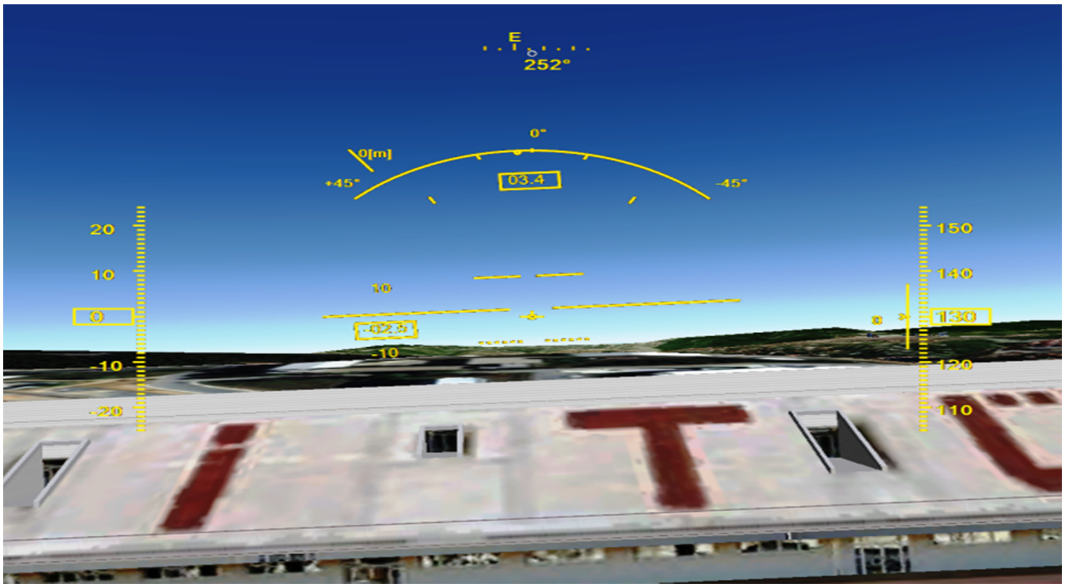

Fig. 24 Synthetic Vision Suite

autonomous missions by adding or editing mission steps such as takeoff, going to waypoints, and landing. The lower left of the GUI has control buttons. Operators can download the mission map from the cache or the Internet, upload flight parameters and view flight parameters in detail with real-time plotting.

Additional software suites such as payload control, synthetic vision, or mission management software can be connected. Figure 24 shows the synthetic vision suite of the ground station software. This add-on program enables the operator to manage the vehicle in poor weather conditions such as foggy weather or during night flights.

5 Ground and Flight Tests

Flight tests and ground were run on the main and subsystems in order to meet the requirements and performance goals. CTOL, VTOL, transition, and autonomous flight tests were completed to ensure the entire system's real-world performance. Ground tests were completed before flight tests to avoid undesirable damage and delay to the project schedule.

For the flight tests, 15 scaled prototypes were manufactured. Figure 25 shows a 1/3-scale TURAC prototype, with the main lift fan and tilt mechanism visible, which are both used for VTOL and transitions tests. Tilts are controlled with the directly mounted high-torque digital servos and all of the motor control systems are independently driven by the autopilot.

Out of the fifteen 1/2 and 1/3 scale prototypes are manufactured for flight tests, nine were built for conventional flight, four for VTOL tests, and two for transition tests.

5.1 Ground Tests

Ground tests were conducted on various TURAC subsystems such as mechanisms and avionics (Fig. 26). Tests were conducted either through a simulated Hardware in the loop environment or through special test

Fig. 25 1/3-scale TURAC prototype

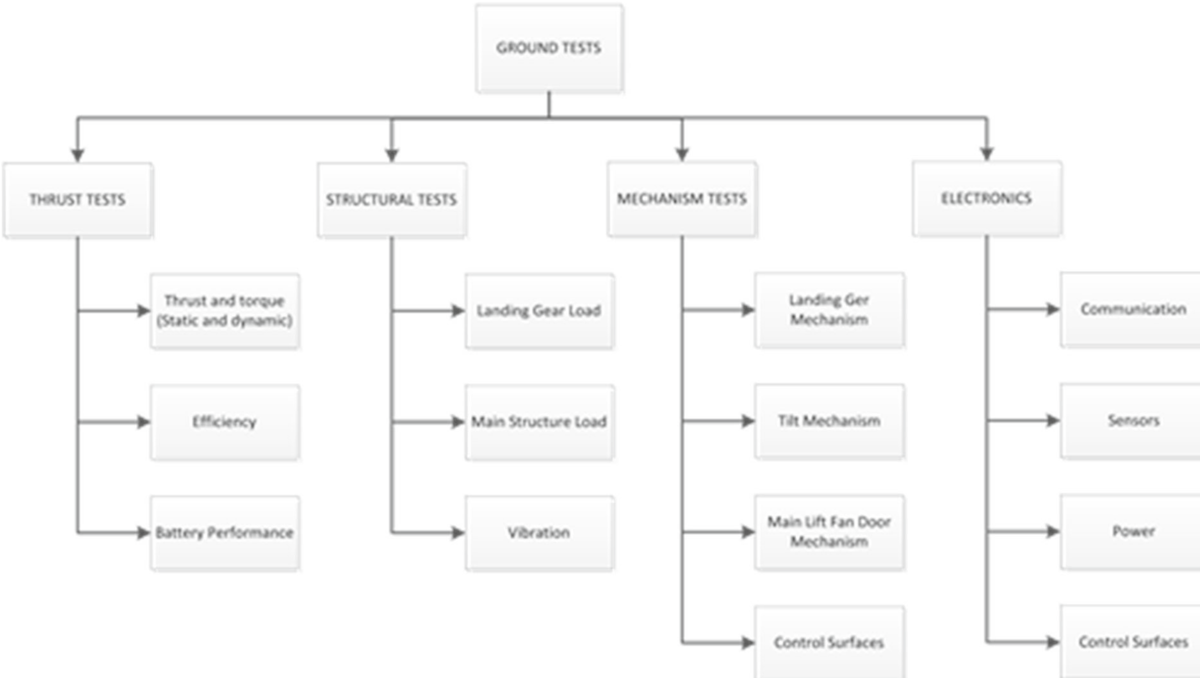

Fig. 26 Ground test plan

equipment such as a thrust test bench and a hydraulic structural tensile test system. The results were used in the design and development stage in order to minimize unwanted interaction of systems and enhance overall performance.

A computer-controlled automatic sequence thrust test bench was designed and built to rapidly and precisely test thrust performance (Fig. 27) through specific parameters such as thrust, torque, RPM, current, voltage, and system efficiency data.

The Thrust Test Bench includes an automatic test sequence which starts with throttle PWM generation (1000–1800). When the sequence starts, data for thrust, torque, RPM, PWM, current, and voltage are recorded. Thrust forces and torque are decomposed with mechanical linkages and connected with independent load cells. Then, resistance differences over load cells are transformed in digital output with the test bench's electronic mainboard. This mainboard also collects data on current, voltage, and RPM sensors, and transforms them into a digital output. Throttle increases automatically step-by-step after 100 readings. Samples are filtered on with Microsoft Excel and the results are used in performance calculations for the next step. Test data is collected on with an Excel spreadsheet and visualized on the test bench's software.

The test bench returns the system response time when the throttle condition is changed. Response time is used for modeling overall control system response. Figure 28 shows the repeated thrust test and simulation with T-motor MT3530 brushless motor and 16x5" carbon propeller. The simulation was modeled with the thrust test bench outputs. Repeated tests show the difference between simulations and tests. Thrust data of tests and simulation are very close until full throttle. After 20 seconds, brushless motor gets hot and the battery loses its performance at maximum discharging rate. At this point, differences between tests and simulation data become greater.

5.2 Flight Tests

Flight tests were used for analyzing the whole system's performance after modifying the subsystems. For this reason, TURAC's performance could be verified in flight tests before the product design. CTOL, VTOL, transition, and autonomous flights were done. All flight tests were performed on 1/2- and 1/3-scale prototypes to reduce the testing budget.

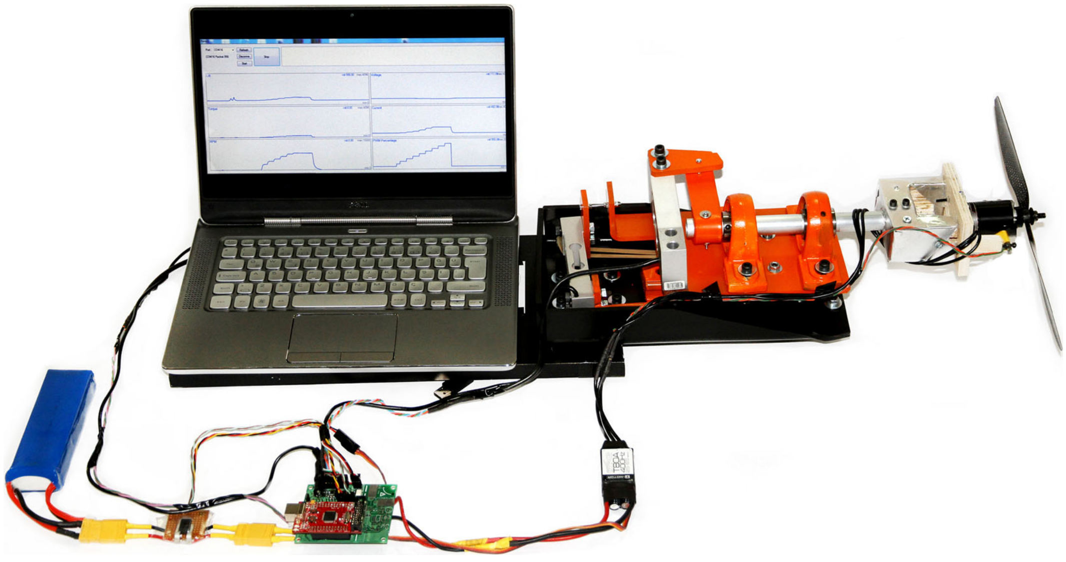

Fig. 27 Thrust test bench

In Table 7, a Flight logbook template is shown which is used for every flight test. Before the test flights, notes were taken on system scale, instruments used on the aircraft, propulsion configuration, and CG location. After tests, opinions and suggestions about the system and tests were taken to solve possible problems and enhance design.

Tested prototypes, versions and test types are tabulated as Table 8. First 2 prototypes for conventional flight were manufactured investigating the aerodynamic similarity of CFD analysis of TURAC V3. First prototype is damaged after take off because of a high crosswind over the runway. Second prototype made its flights and lands safely, but stability and flight performance under expectations which comes from empirical calculations and computer simulations [20]. After investigating the results, laminar flow based airfoils moment coefficient was changed with the turbulent flow which caused from rough airfoil surface of the prototype. Changing the balance of aircraft with flow makes the aircraft almost uncontrollable with pilot inputs.

Fig. 28 Thrust test bench tilt rotor propulsion system for a 1/2-scale TURAC prototype

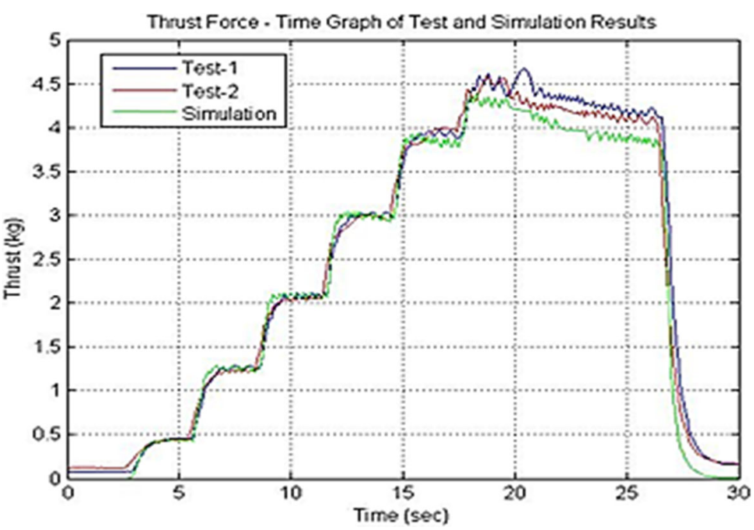

Table 7 Template of flight test logbook of TURAC

Flight Test Logbook of TURAC Systems	
Date/Time	Test time and date information
Location	Test location
Prototype	Prototype number
Scale	Scale of prototype
Take-off Weight	MTOW of prototype
CG Location	Prototype CG location for CG check and stability evaluation
Before Flight Notes	Used systems, battery capacity, modifications and design changes on prototype
Control Mechanisms	Aileron-elevator configuration or elevon configuration
Damage Report	After flight damage report
Repair Report	On the field repairs if prototype is damaged
Test Results	Test objectives and flight characteristics of prototype
Opinions and Suggestions	First evaluation of flight at field
Flight Test Video	Numbered and edited flight videos
Photos	Photos before flight, system arrangement, flight photos and after flight photos. Damage photos are also put in here if prototype is damaged.

TURAC V4 was updated with new airfoil which is more effective in turbulent flow to enhance its stability. New airfoils are also more reliable in wider range of Reynolds number to sustain aerodynamic similarity for scaled prototypes up to 1/3 scale. 2 more prototypes were manufactured to make flight tests. Conventional flight tests were done with predicted performance. After first tests 2 more prototypes are manufactured as VTOL and avionic testbeds. VTOL tests were done at the university stadium and CTOL test were done at the local runway for Radio Controlled (RC) aircrafts. After fifteen CTOL tests aircraft classified as controllable, but aircraft's damping on Dutch roll mode could be increased to make more stable flights without yaw damper.

TURAC V5 was updated with the 5 degree anhedral to increase Dutch roll damping [10]. Moreover, some geometrical modifications are done on the main body to locate main lift fan and its mechanisms. CFD analysis and Matlab simulations are done on full scale and scaled models and Dutch roll damping was increased. On the other hand, logistics became a problem for the team to make flight tests. Moreover, it was getting hard to find COTS parts like brushless motors, ESCs and other parts from local hobby stores in Turkey because of 1/2 scale size. For this reason, 1/3 scale calculations are done on the CFD analysis and Matlab simulations.

Five 1/3 scaled prototypes of conventional TURAC V5 were manufactured and tested successfully. Two VTOL versions of prototypes with fixed rotor mounts were used as avionic testbed at VTOL flight. End of the CTOL and VTOL flight tests two more prototypes with fully controllable tilt mechanisms were

Table 8 Prototype number and test flights

No	Version	Scale	Manufactured Prototype	Test Flight Type	Number of Tests
1	V3	1/2	2	CTOL	6
2	V4	1/2	2	CTOL	15
3	V4	1/2	2	VTOL	11
4	V5	1/3	5	CTOL	28
5	V5	1/3	2	VTOL	13
6	V5	1/3	2	Transition	5

Fig. 29 1/3-scale TURAC completed forward flight tests successfully

manufactured for further transition tests. With the latest two 1/3 prototype, transition tests are successfully done at the university campus as shown in Fig. 31. 1/2 scale transition tests and full scale prototype tests are planned to be done as a future work.

Prototypes of TURAC are equipped with an avionic system which is specially developed for the TURAC platform. T-Motor 3530 motors with 12x7" 3-Blade props by Master Air Screw and T-motor 40A electronic speed controllers are used for the prototypes. A conventional forward flight test is shown in Fig. 29, carried out successfully at Hezarfen Airport.

The TURAC VTOL test with tilt mechanism is shown in Fig. 30. The special tilt mechanism and main lift fan with 12x7" 3-blade counter rotating propeller and independent ESCs were also used as the propulsion unit of a 1/3-scale TURAC prototype. VTOL tests were done at Istanbul Technical University's main campus.

Transition is the most important and challenging issue for fixed-wing VTOLs. Transition flight regime is very complex and the autopilot is required to be capable of handling all aspects of the involved flight regimes. This is because the transition depends on hover and forward flight either at the beginning or at the end of the maneuver. Various transition and back transitions cases were successfully tested on TURAC by using the transition flight control system. Figure 31 shows a transition test in which the flight from hover to forward and vice versa are achieved.

Fig. 30 1/3-scale TURAC VTOL tests in ITU Campus

Fig. 31 Transition maneuver is done successfully with a 1/3-scale TURAC

6 Conclusion

In this paper, we reviewed the design of the TURAC VTOL fixed-wing UAV and detailed a low-cost manufacturing process that allows for efficient and fast prototyping of different variants and designs. The process offers considerable savings in both time and manpower. Given the inherent instability of flight configurations, the operation of the TURAC UAV relies heavily on the automatic flight control system implemented within the avionics system. The ground station with a HUD and synthetic vision provide a highly scalable and user-friendly operation, monitoring, and control. The TURAC UAV is currently undergoing extensive ground and flight tests in which the control system designs for all the operation phases, including hover, transition, and forward flight, are being refined.

Acknowledgments This research is supported in part by the Republic of Turkey, Ministry of Science, Industry, and Technology SANTEZ Program Contract 1585.STZ.2012-2 and HAVELSAN A.S.

References

1. Ozdemir, U., Aktas, Y.O., Vuruskan, A., Dereli, Y., Tarhan, A.F., Demirbağ, K., Erdem, A., Kalaycioglu, G.D., Ozkol, I., Inalhan, G.: Design of a commercial hybrid VTOL UAV system. J. Intell. Robot. Syst. **74**, 371–393 (2014)
2. Karakaş, H., Koyuncu, E., Inalhan, G.: ITU Tailless UAV Design. J. Intell. Robot. Syst. **69**, 131–146 (2013)
3. Aksugur, M., Inalhan, G.: Design Methodology of a Hybrid Propulsion Driven Electric Powered Miniature Tailsitter Unmanned Aerial Vehicle. J. Intell. Robot. Syst. **57**(1–4), 505–529 (2010)
4. Vuruskan, A., Yuksek, B., Ozdemir, U., Yukselen, A., Inalhan, G.: Dynamic Modeling of a VTOL Fix-Wing UAV, ICUAS 2014, Orlando (2014)
5. Mutlu, T., Karaman, S., Comak, S., Bayezit, I., Inalhan, G., Guvenç, L.: Development of a Cross-Compatible Micro-Avionics System for Aerorobotics. In: Proceedings of the IEEE Intelligent Vehicles Symposium, Istanbul, pp. 1258–1265. IEEE (2007)
6. Karaman, S., Aksugur, M., Baltaci, T., Kurtulus, C., Inalhan, G.: Aricopter: Aerobotic Platform for Advances in Flight, Vision Controls, and Distributed Autonomy. In: Proceedings of the IEEE Intelligent Vehicles Symposium, Istanbul, pp. 918–925. IEEE (2007)
7. Ates, S., Bayezit, I., Inalhan, G.: Design and Hardware–in–the–Loop Integration of a UAV Microavionics System in a Manned–Unmanned Joint Airspace Flight Network Simulator. J. Intell. Robot. Syst. **54**, 359–386 (2009)
8. Tarhan, F.A., Koyuncu, E., Hasanzade, M., Inalhan, G.: Formal Intent Based Flight Management System Design for Unmanned Aerial Vehicles, ICUAS 2014, Orlando (2014)
9. Pitera, D.M., DeHaan, M., et al.: Blended Wing Body Concept Development with Open Rotor Engine Integration. NASA GRC and The Boeing Company, Huntington Beach (2011)
10. Nickel, K., Wohlfahrt, M.: Tailless Aircraft in Theory and Practice. AIAA Education Series (1994)
11. Gur, O., Rosen, A.: Optimizing Electric Propulsion Systems for Unmanned Aerial Vehicles. J. Aircr. **46**(4), 1340–1353 (2009)
12. Yuksek, B., Vuruskan, A., Ozdemir, U., Yukselen, A., Inalhan, G.: Dynamic Modeling of a Fixed-Wing VTOL UAV. In: Proceeding of 2015 International Conference on Unmanned Aircraft Systems
13. Dereli, Y.: Structural Modeling and Analysis of TURAC Unmanned Air Vehicle, MSc. Thesis, Istanbul Technical University (2014)
14. Zhao, H.W.: Development of a Dynamic Model of a Ducted Fan VTOL UAV. MSc, Thesis, RMIT University (2009)
15. Boddington, D.: Building & Flying Radio Controlled Model Aircraft, Special Interest Model Books (2005)
16. Lennon, A.: Basics of R/C Model Aircraft Design, Practical Techniques for Building Better Models, Air Age (1996)
17. Campell, F.C.: Manufacturing Technology for Aerospace Structural Materials. Elsevier (2006)
18. Rae, A.: Prototyping Overview, Product Design and Development Lecture Notes, Massachusetts Institute of Technology
19. Yagnik, D.: Fused Deposition Modelling - A Rapid Prototyping Technique for Product Cycle Time Reduction Cost Effectively in Aerospace Applications. International Conference on Advances in Engineering and Technology (ICAET), pp. 62–68 (2014)
20. Kimberlin, R.D.: Flight Testing of Fixed-Wing Aircraft. AIAA Education Series (2003)